

2000

Air-Side Thermal Performance of Micro-Channel Heat Exchangers Under Dehumidifying Conditions

M. H. Kim

University of Illinois at Urbana-Champaign

C. W. Bullard

University of Illinois at Urbana-Champaign

Follow this and additional works at: <http://docs.lib.purdue.edu/iracc>

Kim, M. H. and Bullard, C. W., "Air-Side Thermal Performance of Micro-Channel Heat Exchangers Under Dehumidifying Conditions" (2000). *International Refrigeration and Air Conditioning Conference*. Paper 473.
<http://docs.lib.purdue.edu/iracc/473>

This document has been made available through Purdue e-Pubs, a service of the Purdue University Libraries. Please contact epubs@purdue.edu for additional information.

Complete proceedings may be acquired in print and on CD-ROM directly from the Ray W. Herrick Laboratories at <https://engineering.purdue.edu/Herrick/Events/orderlit.html>

AIR-SIDE THERMAL PERFORMANCE OF MICRO-CHANNEL HEAT EXCHANGERS UNDER DEHUMIDIFYING CONDITIONS

Man-Hoc Kim and Clark W. Bullard

Department of Mechanical and Industrial Engineering, University of Illinois at Urbana-Champaign
140 MEB, MC-244, 1206 West Green Street, Urbana, IL 61801

ABSTRACT

An experimental study for air-side thermal-hydraulic performance of brazed aluminum heat exchangers under dehumidifying conditions has been performed. For 30 samples of louvered fin heat exchangers with different geometrical parameters, the heat transfer and pressure drop characteristics for wet surface were evaluated. The test was conducted for air-side Reynolds number in the range of 80-300 and tube-side water flow rate of 320kg/h. The dry- and wet-bulb temperatures of the inlet air for heat exchangers were 27°C and 19°C, respectively and the inlet water temperature was 6°C. The air-side thermal performance data for cooling and dehumidifying conditions were analyzed using effectiveness-NTU method for cross-flow heat exchanger with both fluids unmixed. The test results were reported, compared with those for the dry surface heat exchangers, in terms of sensible j-factor and friction factor f , as functions of Reynolds number based on louver pitch. The correlations for j and f factors are developed within rms errors of 16.9 and 13.6 %, respectively.

NOMENCLATURE

<p>A_c : Minimum free-flow area for air side, m²</p> <p>A_f : Fin surface area, m²</p> <p>A_{fr} : Frontal area, m²</p> <p>A_{ow} : Total air-side surface area, m²</p> <p>A_t : External tube surface area, m²</p> <p>A_w : Tube wall area, m²</p> <p>c_p : Specific heat, J/kgK</p> <p>Cr : Capacity ratio</p> <p>D_h : Hydraulic diameter, m</p> <p>f : Fanning friction factor</p> <p>F_p : Fin pitch, m</p> <p>F_d : Flow depth, m</p> <p>H : Fin height, m</p> <p>h : Heat transfer coefficient, W/ m²K</p> <p>h_{ow} : Total heat transfer coefficient, W/ m²K</p> <p>h_o : Sensible heat transfer coefficient, W/ m²K</p> <p>j : Colburn j-factor ($Nu/Re Pr^{1/3}$)</p> <p>k : Thermal conductivity, W/mK</p> <p>k_{al} : Thermal conductivity of tube wall, W/mK</p> <p>Kc : Abrupt contraction coefficient</p> <p>Ke : Abrupt expansion coefficient</p> <p>l : Fin length, m</p> <p>L_α : Louver angle, deg</p> <p>L_l : Louver length, m</p> <p>L_p : Louver pitch, m</p> <p>\dot{m} : Mass flow rate, kg/s</p> <p>m^* : Refer Eq(11), m⁻¹</p> <p>Nu : Nusselt number (hD/k)</p> <p>P : Pressure drop, Pa</p> <p>Pr : Prandtl number (ν/α)</p> <p>Q : Heat transfer rate, W</p> <p>Re : Reynolds number</p>	<p>Re_{LP} : Reynolds number based on louver pitch</p> <p>T : Temperature, K</p> <p>T_d : Tube depth, m</p> <p>T : Temperature difference, K</p> <p>$U_{ow}A_{ow}$: Overall thermal conductance, W/K</p> <p>V_c : Maximum air velocity, m/s</p> <p style="text-align: center;">Greek letters</p> <p>α : Louver angle, deg</p> <p>γ : Aspect ratio of tube hole</p> <p>δ_f : Fin thickness, m</p> <p>δ_w : Tube wall thickness, m</p> <p>ε : Effectiveness</p> <p>η_{fw} : Fin efficiency</p> <p>η_{ow} : Surface effectiveness</p> <p>ρ : Density, kg/m³</p> <p>ρ_m : Mean average air density, kg/m³</p> <p>σ : Contraction ratio of the fin array (A_c/A_f)</p> <p style="text-align: center;">Subscripts</p> <p>ave : Average value</p> <p>1 : Inlet for air side</p> <p>2 : Outlet for air side</p> <p>i : Water side</p> <p>l : Louver</p> <p>max : Maximum value</p> <p>min : Minimum value</p> <p>o : Air side</p> <p>t : Tube</p> <p>w : Tube wall or water</p> <p>ow : Wet surface</p>
--	---

INTRODUCTION

Heat exchangers play an important role in the energy efficiency and physical size of the refrigeration and air conditioning system. Heat exchangers in refrigeration and air conditioning applications are classified as a condenser and an evaporator and finned round tube heat exchangers are used extensively. Improving the technology of heat exchanger performance, particularly air-side performance, has attracted many investigators [1-3]. Since the surface of the evaporator is subject to condensation of moisture contained in air in cooling mode operation, the design of air-side configuration of the heat exchanger requires consideration of heat and mass transfer simultaneously. Research on the air-side thermal performance of finned tube heat exchangers under wet condition has been performed by several investigators [4-18].

McQuiston [4-6] studied heat and mass transfer on wet coils and developed correlations for the heat transfer coefficients and pressure drops. Threlkeld [7], McQuiston [8], and Wu and Bong [9] provided the fin efficiency for the fully wet surface heat exchangers. Wu and Bong also presented the overall fin efficiency for the partially wet surface, and reported that only when the fin is partially wet the overall fin efficiency depends significantly on the relative humidity. Hill and Jeter [10] developed a linear sub-grid model for the air conditioner's cooling and dehumidifying coil which is an evaporator. They showed the single-pass, cross flow arrangement of the model was adequate to model counter cross flow heat exchangers. Mirth et al. [11] investigated performance analysis of the cooling coil based on ARI Standard [12] and Hu et al. [13] presented the effect of the shape of the condensation water on the fin surface on thermal performance characteristics. Youn et al. [14] and Domanski and Didion [15] proposed a model to analyze the performance for various air conditioning evaporators based on tube-by-tube method, and reported that the sensible heat transfer coefficient for wet surface was larger than that for dry surface. On the other hand, Wang et al. [16] reported the heat transfer coefficient for wet surface is smaller than that of dry surface based on a study on the thermal-hydraulic performance of the dehumidifying coil. Chuah et al. [17] investigated dehumidifying performance of chilled water coils with variation of water flow rate. Kim and Jacobi [18] investigated condensation accumulation effects on air-side heat transfer and pressure drop characteristics for plain and slit fins and round tube heat exchangers. However, there are few data on the air-side performance for louvered fin brazed aluminum heat exchangers with dehumidification.

Webb and Jung [19] carried out one study for applying the brazed aluminum heat exchangers to the residential air conditioner, and showed heat transfer rate of the brazed aluminum heat exchanger was 50% higher than that of conventional heat exchanger. They reported drainage of condensation water on the heat exchanger surface could be removed well and it could be used as an evaporator for the residential air conditioning system. Chiou et al. [20] investigated thermal performance of serpentine type automotive evaporator with flat tube and louvered fins. They reported that the sensible heat transfer coefficient for wet surface was larger than that for dry surface. However, there is no published data in the open literature for the correlations of j and f factors of brazed aluminum heat exchangers under wet condition.

This study presents the heat transfer and pressure drop behaviors of brazed aluminum heat exchangers under wet surface condition. A series of tests are conducted for the heat exchangers with several different air-side configurations such as louver angle, flow depth, and fin density. Test results are compared with those for dry surface, and sensible j -factor and friction factor f are reported as functions of Reynolds number based on louver pitch, and correlations for the j and f factors are extracted from the test data.

EXPERIMENTS

Test apparatus

Figure 1 shows a schematic diagram of the test apparatus used in the study. It consists of a suction type wind tunnel, heat transfer fluid (water) circulation and control units, and data acquisition system and is situated in a constant temperature and humidity chamber. The air inlet condition of the heat exchanger can be maintained by controlling the chamber temperature and humidity. The air inlet and outlet dry and wet bulb temperatures for the heat exchanger are measured associated with sampling units. The air-side pressure drop through the heat exchanger is measured using a differential pressure transducer and air flow rate is measured using nozzle pressure difference. The heat transfer fluid circulation and control units can maintain the inlet condition of water-side by regulating water flow rate and inlet temperature. The uncertainty of heat transfer rate for the test apparatus is within 3% since accuracy of

temperature measurement is $\pm 0.1^\circ\text{C}$ and accuracy of air and water flow rates are $\pm 1\%$ and $\pm 2\%$, respectively.

Test heat exchangers

Figures 2 and 3 indicate geometrical configuration and terminology of the test heat exchanger. The heat exchangers are louvered fin and micro-channel heat exchangers; 30 heat exchanger samples are used for the test. Table 1 shows simple specification of the test heat exchangers. Fin pitches are 1.2, and 1.4 mm for all cases, plus 1.0 mm for heat exchangers of louver angle 23° with flow depth of 16 and 24 mm. Louver pitch, louver length and fin height are 1.7 mm, 6.4 mm and 8.15 mm, respectively, and core size of heat exchangers is 350x 255 mm.

Test condition and method

The heat exchanger is installed in the test section and insulation is placed around heat exchanger to protect it from heat loss and air leakage. The tests are performed in range of Reynolds number of 80-400 with water flow rate maintained at 320 kg/h. The inlet air dry and wet bulb temperatures of the heat exchangers are maintained at 27°C and 19°C , respectively, and the inlet water temperature is 6°C .

Data reduction

When a heat exchanger is used as an evaporator, it is subjected to accumulation of condensation water when its surface temperature is below the dew point of the inlet air. The analysis of wet heat exchangers requires consideration of heat and mass transfer simultaneously. Moist air properties required for analysis of the test data are calculated based on ASHRAE Handbook [21].

Heat transfer rate required for calculation of air-side heat transfer coefficient can be expressed as

$$Q = (Q_o + Q_i) / 2 \quad (1)$$

Where Q_o and Q_i are heat transfer rates of air and water sides, respectively. The approach used here for data reduction, employs the total enthalpy method for moist air calculations [21]. It assumes that air behaves as a non-reacting ideal mixture with water vapor as a dilute component, which introduces small errors at these conditions.

$$Q_o = \dot{m}_o [1.006(t_{db,1} - t_{db,2}) + 1.805(W_1 t_{db,1} - W_2 t_{db,2})] + 2501 \dot{m}_o (W_1 - W_2) \quad (2)$$

$$Q_i = \dot{m}_i c_{p,i} (t_{i1} - t_{i2}) \quad (3)$$

The first and second terms of the right hand side of the equation (2) indicate sensible and latent heat, respectively. Effectiveness and NTU method can be used for obtaining air-side heat transfer coefficient. The equation for both fluids unmixed is

$$\varepsilon = 1 - \exp \left[\frac{-NTU^{0.22}}{C_r} \left\{ \exp(-C_r NTU^{0.78}) - 1 \right\} \right] \quad (4)$$

Effectiveness and NTU for the wet heat exchanger can be expressed

$$\varepsilon = Q / Q_{\max}, \quad NTU = U_{ow} A_{ow} / \dot{m}_o, \quad Cr = \frac{\dot{m}_o b_w}{\dot{m}_i c_{p,o}} \quad (5)$$

where Q_{\max} and b_w are

$$Q_{\max} = \dot{m}_o (i_{o1} - i_{s,i1}), \quad i_s = a_w + b_w t_s \quad (6)$$

The overall heat transfer coefficient for wet surface is given by:

$$\frac{1}{U_{ow}A_{ow}} = \frac{b'_i}{h_iA_i} + \frac{b'_p\delta_{wal}}{k_{wal}A_{wal}} + \frac{b_w}{\eta_{ow}h_{ow}A_{ow}} \quad (7)$$

$$b'_i = \frac{i_{s,Pi} - i_{s,i}}{t_{Pi} - t_i}, \quad b'_p = \frac{i_{s,Po} - i_{s,Pi}}{t_{Po} - t_{Pi}} \quad (8)$$

For heat transfer coefficients of water-side, the following equation is developed based on test results [22] obtained for the same micro-fin tubes used this study.

$$Nu_i = Nu_{ref} + 0.0499 Re_i Pr_i \frac{D_{hi}}{L} \quad (9)$$

$$Nu_{ref} = 7.541(1 - 1.969\gamma + 5.664\gamma^2 - 12.866\gamma^3 + 19.349\gamma^4 - 16.197\gamma^5 + 5.51\gamma^6)$$

Where Nu_{ref} is derived using Schmidt's data [23] of rectangular ducts with different aspect ratios γ . The surface effectiveness and fin efficiency for wet surface [7] are

$$\eta_{ow} = 1 - \frac{A_f}{A_{ow}}(1 - \eta_{fw}) \quad (10)$$

$$\eta_{fw} = \frac{\tanh(m^*l)}{m^*l}, \quad m^* = \sqrt{\frac{2h_{ow}}{k_f\delta_f} \left(1 + \frac{\delta_f}{F_d}\right)}, \quad l = H/2 - \delta_f \quad (11)$$

Heat transfer coefficient for wet surface is

$$h_{ow} = \frac{1}{\frac{c_{p,o}}{b_w h_o} + y_w/k_w} \quad (12)$$

where h_o is the sensible heat transfer coefficient for wet surface, and y_w is the thickness of condensation water film, which is assumed as 0.1 mm [24].

Then we can estimate pressure drop in the control volume using the above information

$$j = \frac{h_{co}}{\rho_m V_c c_{p,o}} Pr_o^{2/3} \quad (13)$$

$$f = \frac{A_c}{A} \frac{\rho_m}{\rho_1} \left[\frac{2\rho_1 \Delta P}{(\rho_m V_c)^2} - (K_c + 1 - \sigma^2) - 2 \left(\frac{\rho_1}{\rho_2} - 1 \right) + (1 - \sigma^2 - K_e) \frac{\rho_1}{\rho_2} \right] \quad (14)$$

Where K_c and K_e are coefficients for pressure loss at the inlet and outlet of the heat exchanger.

RESULTS AND DISCUSSION

Figures 4-7 present the test results for aluminum micro-channel heat exchangers with louvered fin. For $Fp=1.4$ mm and $L\alpha=23^\circ$, Figure 4 (a) shows variations of sensible heat transfer coefficient and pressure drop with face air velocity and flow depth. Heat transfer coefficient increases with increasing frontal air velocity and decreasing flow

depth because of decreasing of boundary layer thickness, while pressure drop increases as expected. Figure 4(b) shows how sensible heat transfer coefficient and pressure drop vary with louver angle for a face air velocity of 1.0 m/s, compared to those for dry condition [25]. Sensible heat transfer coefficients for wet surface are smaller than those for dry condition over the entire range of operating conditions, while pressure drops are larger. This behavior may be explained partly as follows; condensation water on surface acts as thermal resistance for the relatively low air velocity, typical of residential air conditioning systems [13]. It was observed that heat transfer coefficient decreases when louver angle is larger than 27°, since flow efficiency decreases beyond a certain louver angle. Pressure drops for wet surface are 3-30% higher than those for dry surface, especially at the lowest louver angle where condensate bridging between louvers may significantly impair heat transfer and increase the amount of condensate retained. For smaller fin pitch, the difference between pressure drops for dry and wet surfaces is larger because difficulty for drainage of condensation water may increase with decreasing fin pitch. Except for the smallest (15°) louver angle, the overall characteristics of thermal performance with respect to louver angle for wet surface are similar to those for dry surface.

Figure 5 depicts heat transfer rate versus fan power for $F_p=1.4$ mm with different louver angles and flow depths. Ideal fan power is calculated using face air velocity (u), face area of heat exchanger (A_f) and pressure drop through heat exchanger (ΔP)

$$P_{fan} = uA_f \Delta P \quad (15)$$

As shown in the figure, heat transfer rate has a maximum value for $L\alpha=19-23^\circ$ in case of $F_d=20$ mm, while it has a maximum value for $L\alpha=27^\circ$ in case of $F_d=24$ mm. This suggests the existence of an optimal louver geometry for a given system operation condition.

Figure 6 presents Colburn j factor and friction factor f as functions of Reynolds number based on louver pitch, compared to those for dry surface [25]. The effect of Reynolds number on heat transfer coefficient in the low Reynolds number region is larger than that in the high Reynolds number region. That means the effect of condensation water on heat transfer performance decreases as Reynolds number increases. As shown in the Figure for $L\alpha=27^\circ$, j factor for wet surface is smaller than that for dry surface at low Reynolds number, while it is larger than that for dry surface at large Reynolds number. This behavior is consistent with the result of Hu et al. [13] who reported that at low Reynolds number condensation water increased thermal resistance, and so heat transfer decreased, while at high Reynolds number condensation generated streamwise vorticity, and the increased mixing improved heat transfer performance. Friction factor for wet surface increases with increasing louver angle as expected.

Correlations for j and f factors are developed using 129 data points with rms errors of 16.9 % and 13.6%, respectively:

$$j = \text{Re}^{-0.512} \left(\frac{L\alpha}{90}\right)^{0.25} \left(\frac{F_p}{L_p}\right)^{-0.171} \left(\frac{H}{L_p}\right)^{-0.29} \left(\frac{T_d}{L_p}\right)^{-0.248} \left(\frac{L_l}{L_p}\right)^{0.68} \left(\frac{T_p}{L_p}\right)^{-0.275} \left(\frac{\delta_f}{L_p}\right)^{-0.05} \quad (16)$$

$$f = \text{Re}^{-0.798} \left(\frac{L\alpha}{90}\right)^{0.395} \left(\frac{F_p}{L_p}\right)^{-2.635} \left(\frac{H}{L_p}\right)^{-1.22} \left(\frac{T_d}{L_p}\right)^{0.823} \left(\frac{L_l}{L_p}\right)^{1.97}$$

Figures 8 and 9 compare these to other correlations for two different types of heat exchangers as shown in Table 2. For both heat exchangers, j factors for wet surface are consistently smaller than those for dry surface [25-26]. For heat exchanger type-I, f factors are larger than those for dry surface [25, 27] as expected. However, for heat exchanger type-II, which has relatively large flow depth, f factor is similar to that of the same heat exchangers under dry condition [25] and larger than that of Chang et al.'s correlation [27].

CONCLUSION

The heat transfer and pressure drop characteristics for louvered fin micro-channel heat exchangers under dehumidifying conditions have been investigated using 30 different heat exchanger samples. At low Reynolds

number, the sensible heat transfer coefficient for wet surface is smaller than that of the same heat exchanger for dry surface. As Reynolds number increases, however, the sensible heat transfer coefficients for wet surface increase and is similar to that for dry surface. The pressure drop for wet surface is consistently higher than that for dry surface. The correlations for j and f factors are developed within rms errors of 16.9 % and 13.6%, respectively. The correlations proposed here predicted well test data for the heat exchangers having different configurations.

ACKNOWLEDGEMENTS

We are grateful for supporting of this study to Samsung Electronics Co., Ltd. and the 25 member companies of the Air Conditioning and Refrigeration Center (ACRC) at the University of Illinois at Urbana-Champaign.

REFERENCES

1. A.M. Jacobi and R.K. Shah, 1998, Air-side flow and heat transfer in compact heat exchangers: A discussion of enhancement mechanisms, *Heat Transfer Engineering*, Vol. 19, No. 4, pp. 1-13.
2. R.L. Webb, 1998, Advances in air-cooled heat exchanger technology, Proceedings of International Conference on Heat Exchanger for Sustainable Development, Lisbon, Portugal, pp. 677-692.
3. N.C. DeJong and A.M. Jacobi, 1999, Flow, heat transfer, and pressure drop interactions in louvered-fin arrays, ACRC TR-146.
4. F.C. McQuiston, 1976, "Heat, mass and momentum transfer in a parallel plate dehumidifying exchanger," *ASHRAE Trans.*, Vol. 82, Pt. 1, pp. 82-106.
5. F.C. McQuiston, 1978, "Heat, mass and momentum transfer data for five plate-fin-tube heat transfer surface," *ASHRAE Trans.*, Vol. 84, Pt. 1, pp. 266-293.
6. F.C. McQuiston, 1978, "Correlation of heat, mass and momentum transport coefficients for plate-fin-tube heat transfer surfaces with staggered tubes," *ASHRAE Trans.*, Vol. 84, Pt. 1, pp. 294-308.
7. T.H. Kuehn, J.W. Ramsey, and J.L. Threlkeld, 1998, *Thermal environmental engineering*, 3rd ed., Prentice Hall, pp. 289-331.
8. F.C. McQuiston, 1975, "Fin efficiency with combined heat and mass transfer," *ASHRAE Trans.*, Vol. 81, Pt. 1, pp. 350-355.
9. G. Wu and T.-Y. Bong, 1994, "Overall efficiency of a straight fin with combined heat and mass transfer," *ASHRAE Trans.*, Vol. 100, Pt. 1, pp. 367-374.
10. J.M. Hill and S.M. Jeter, 1991, A linear subgrid cooling and dehumidification coil model with emphasis on mass transfer," *ASHRAE Trans.*, Vol. 97, Pt. 2, pp. 118-128.
11. D.R. Mirth, S. Ramadhyani, and D.C. Hittle, 1993, "Thermal performance of chilled-water cooling coils operating at low water velocities," *ASHRAE Trans.*, Vol. 99, pp. 43-53.
12. ARI Standard 410-91, 1991, Forced circulation air-cooling and air-heating coils, ARI, Arlington, VA, U.S.A.
13. X.Hu, L. Zhang, and A.M. Jacobi, 1994, "Surface irregularity effects of droplets and retained condensate on local heat transfer to finned tubes in cross-flow," *ASHRAE Trans.*, Vol. 100, Pt. 1, pp. 375-381.
14. Youn, B., Yoo, K.C., Park, H.Y., and Kim, Y.S., 1996, "Modeling of cross-flow fin-tube evaporator," Proceedings of KSME Conference – Thermal Fluid division, pp. 73-81.
15. Domanski, P.A., and Didion, D.A., 1983, "Computer modeling of the vapor compression cycle with constant flow area expansion device," NBS Building Science Ser. 155, NIST.
16. C. Wang, Y. Hsieh, and Y. Lin, 1997, "Performance of plate finned tube heat exchangers under dehumidifying conditions," *Trans. of ASME, J. of Heat Transfer*, Vol. 119, pp. 109-117.
17. Kim, G.J. and Jacobi, A.M., 2000, "Condensate accumulation effects on the air-side thermal performance of slit-fin surfaces," ACRC Report CR-26, University of Illinois at Urbana-Champaign.
18. Y.K. Chuah, C.C. Hung, and P.C. Tseng, 1998, "Experiments on the dehumidification performance of a finned tube heat exchangers," *HVAC&R Research*, Vol. 4, No. 2, pp. 167-178.
19. R. L. Webb and S. H. Jung, 1992, Air-side performance of enhanced brazed aluminum heat exchangers, *ASHRAE Trans.*, Vol. 98, Pt. 2, pp. 391-401.
20. C.B. Chiou, C.C. Wang, Y.J. Chang, and D.C. Lu, 1994, Experimental study of heat transfer and flow friction characteristics of automotive evaporators, *ASHRAE Trans.*, Vol. 100, Pt. 2, pp. 575-581.
21. *ASHRAE Handbook*, 1997, Fundamentals, pp. 6.1-6.17.
22. Kim, N.-H., 1998, Private communications, University of Incheon, Incheon, Korea.
23. Shah, R. K. and London, A. L., 1978, *Laminar flow forced convection in ducts*, Academic Press, pp. 247-252.
24. Myers, R.J., 1967, "The effect of Dehumidification on the air-side heat transfer coefficient for a finned tube coil," M.S. Thesis, University of Minnesota, Minneapolis.
25. Kim, M.-H. And Bullard, C.W., 2000, "Air-side heat transfer and pressure drop characteristics of micro-channel heat exchangers," Submitted to Int. Mechanical Engineering Congress & Exposition, Advanced Energy Systems Division, Orlando.
26. Chang, Y. and Wang, C., 1997, "A generalized heat transfer correlation for louvered fin geometry," *Int. J. Heat Mass Transfer*, Vol. 40, No. 3, pp. 533-544.
27. Chang, Y., Wang, C. and Chang, W., 1994, "Heat Transfer and Flow Characteristics of Automotive Brazed Aluminum Heat Exchangers," *ASHRAE Trans.*, Vol. 100, Part 2, pp. 643-652.

Table 1. Specification of the test heat exchangers

Flow depth (F_d , mm)	Tube pitch (T_p , mm)	Number of louvers	Louver angle (L_a , °)
16	11.15	8	23, 25, 27, 29
20	10.15	10	15, 19, 23, 27
24	10.15	12	23, 25, 27, 29

Table 2 Heat exchanger samples for comparison of correlations

Heat exchanger type	L_a (°)	F_p (mm)	L_p (mm)	L_1 (mm)	H (mm)	T_p (mm)	T_d (mm)	δ_f (mm)
I	23	1.4	1.7	6.4	8.15	10.15	16	0.1
II	30	1.6	1.55	7.16	8.8	10.24	41.76	0.1

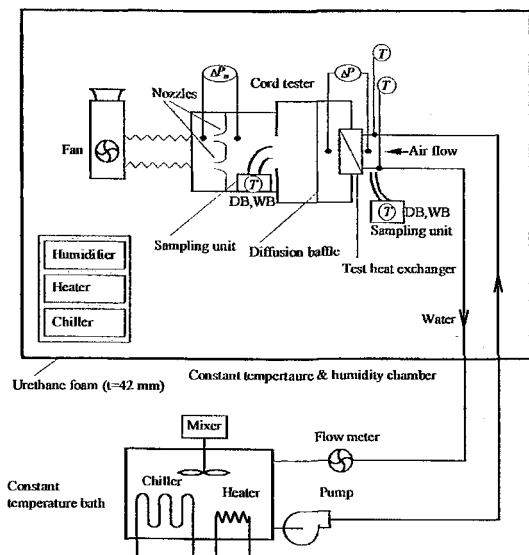


Figure 1. Schematic diagram of test apparatus

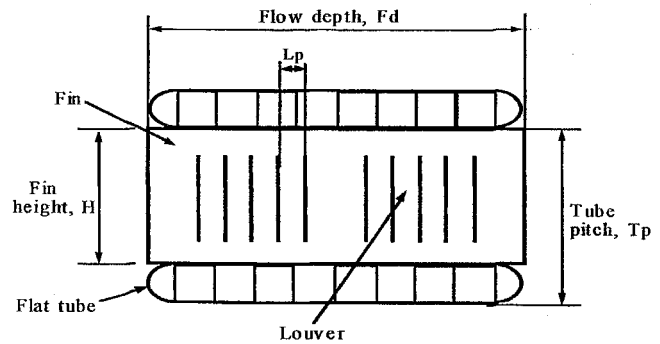


Figure 2. Definition of geometric parameters

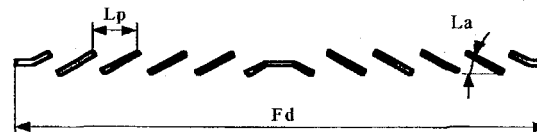
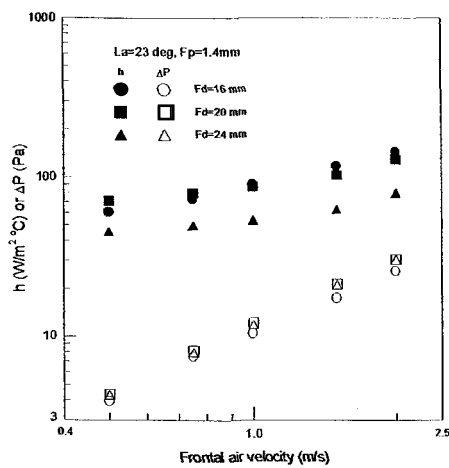
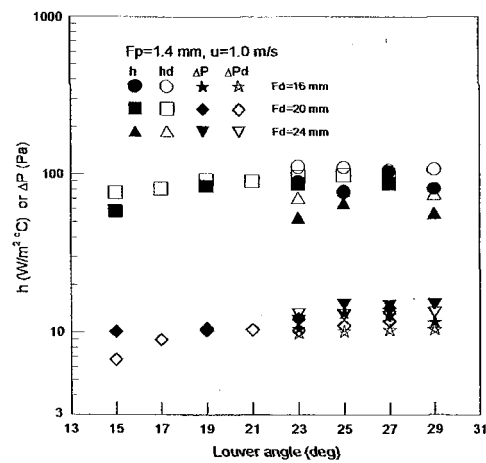


Figure 3. Cross section of louver fin geometry



(a) for $L_a=23^\circ$ and $F_p=1.4$ mm



(b) for $u=1.0$ m/s and $F_p=1.4$ mm

Figure 4. Sensible heat transfer coefficient and pressure drop

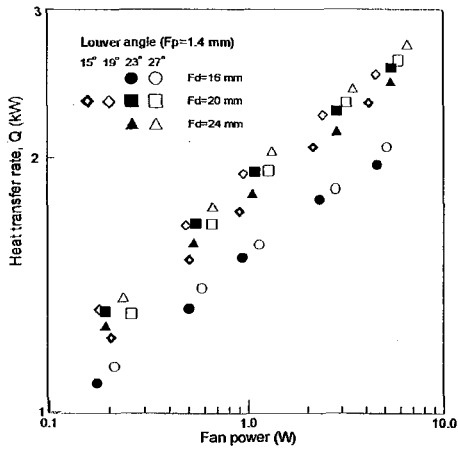


Figure 5. Heat transfer rate vs. fan power

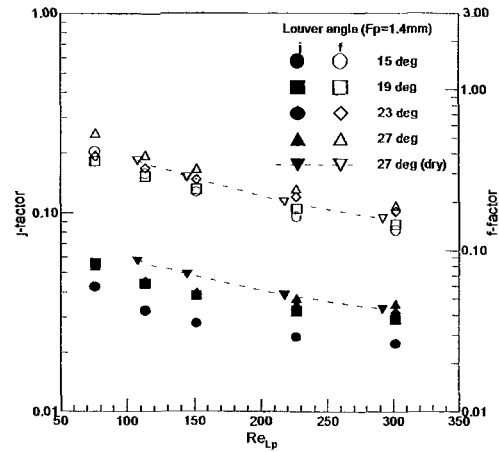
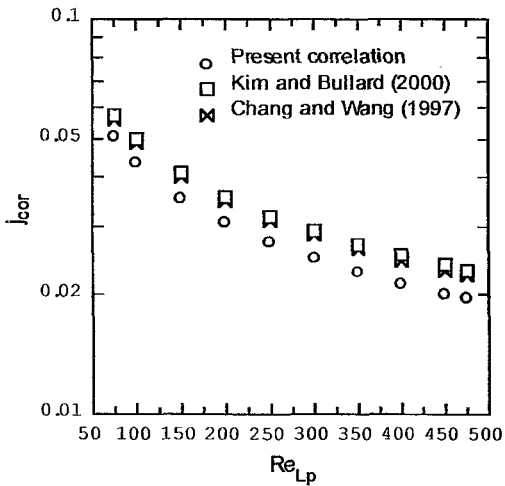
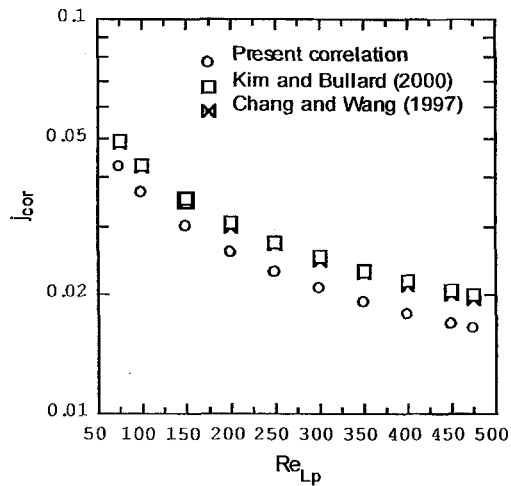


Figure 6. j and f factors for $F_d = 20$ mm

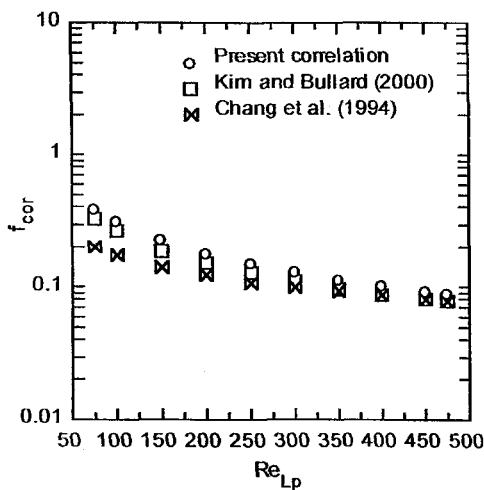


(a) Heat exchanger type-I

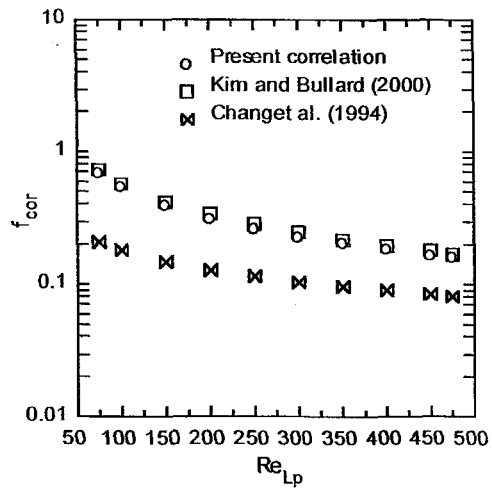


(b) Heat exchanger type-II

Figure 7. Comparison of present and other correlations for j-factor



(a) Heat exchanger type-I



(b) Heat exchanger type-II

Figure 8. Comparison of present and other correlations for f-factor